0026-895X/99/030497-11$3.00/0

MOLECULAR PHARMACOLOGY, **55:**497–507 (1999).

Identification and Characterization of Multiple Subtypes of Muscarinic Acetylcholine Receptors and Their Physiological Functions in Canine Hearts

HONG SHI, HUIZHEN WANG, and ZHIGUO WANG

Department of Medicine, University of Montreal, Montreal, Quebec, Canada (Z.W.), and Research Center, Montreal Heart Institute, Montreal, Quebec, Canada (H.S., H.W., Z.W.)

Received June 1, 1998; accepted December 7, 1998

This paper is available online at http://www.molpharm.org

ABSTRACT

M_2 receptors have long been believed to be the only functional subtype of muscarinic acetylcholine receptor (mAChR) in the heart, although recent studies have provided evidence for the presence of other subtypes. We performed a detailed study to clarify this issue. In the presence of tetramethylammonium (1 μM to 10 mM), a novel K^+ current with both delayed rectifying and inward rectifying properties (I_{KTMA}) was activated in single canine atrial myocytes. 4-Aminopyridine (0.05–2 mM) also induced a K^+ current (I_{K4AP}) with characteristics similar to but distinct from those of I_{KTMA}. Both I_{KTMA} and I_{K4AP} were abolished by 1 μM atropine. I_{K4AP}, but not I_{KTMA}, was minimized by treatment with pertussis toxin. I_{KTMA} was markedly decreased by 4-diphenylacetoxy-*N*-methylpiperidine methiodide (a selective antagonist for M_3 subtype) but was not altered by pirenzepine (for M_1), methoctramine (for M_2), and tropicamide (for M_4). Tropicamide substantially reduced I_{K4AP}, but the antagonists for other mAChR subtypes had no effects on I_{K4AP}. By comparison, I_{KACh} (ACh-induced K^+ current) was significantly depressed by methoctramine but was unaltered by other antagonists. Results from displacement binding of [*methyl*-^{3}H]*N*-scopolamine methyl chloride with pirenzepine, methoctramine, 4-diphenylacetoxy-*N*-methylpiperidine methiodide, or tropicamide revealed the coexistence of multiple mAChR subtypes in canine atrium. Cloning of cDNA fragments and detection of mRNAs coding for M_2, M_3, and M_4 provided further supporting evidence. Our results suggest that 1) multiple subtypes of mAChRs (M_2/M_3/M_4) coexist in the dog heart and 2) different subtypes of mAChRs are coupled to different K^+ channels. Our findings represent the first functional evidence for the physiological role of cardiac M_3 and M_4 receptors.

Accumulating evidence indicates that the functional responses of cells to muscarinic acetylcholine receptors (mAChRs) are mediated by multiple receptor subtypes (Hulme et al., 1990; van Zwieten and Doods, 1995). The heterogeneity of mAChR was first suggested on the basis of pharmacological profiles (differential binding affinity and functional studies) of receptor agonists and antagonists (Goyal, 1989; Hulme et al., 1990). To date, at least four different subtypes have been pharmacologically and functionally defined in primary tissues, designated M_1, M_2, M_3, and M_4 (Eglen and Whiting, 1990; Mutschler et al., 1995; van Zwieten and Doods, 1995). Five isoforms of mAChR have been identified based on molecular cloning studies, designated m_1 through m_5, each of which is encoded by an intronless gene with unique amino acid sequence and distinct tissue distribution (Bonner et al., 1987; Peralta et al., 1987; Goyal, 1989). Four of these cloned subtypes (m_1, m_2, m_3, and m_4) correspond to the functional receptors M_1, M_2, M_3, and M_4, whereas the physiological relevance of m_5 remains to be established.

The M_2 receptor is commonly believed to be the only functional mAChR subtype in the heart (Watson et al., 1983; Bonner et al., 1987; Mizushima et al., 1987; Peralta et al., 1987) and contributes to the regulation of the heart rate and contractility and to shaping of the action potentials (Jeck et al., 1988; van Zwieten and Doods, 1995). Binding of acetylcholine (ACh) to mAChRs in cardiac cells is known to induce an inward rectifier potassium current (I_{KACh}). This action of ACh is mediated by M_2 receptors coupled to I_{KACh} via G_i protein (Yatani et al., 1988; Takano and Noma, 1997). Recent

[1] This work was supported in part by the Medical Research Council of Canada, the Heart and Stroke Foundation of Quebec, an Establishment Grant for young investigators from the Fonds de Recherche en Santé du Québec (Z.W.), and the Fonds de Recherche de l'Institut de Cardiologie de Montréal. Z.W. is a Heart and Stroke Foundation of Canada Research Scholar.

ABBREVIATIONS: mAChR, muscarinic acetylcholine receptor; ACh, acetylcholine; TMA, tetramethylammonium; I_{KTMA}, tetramethylammonium-induced K^+ currents; PTX, pertussis toxin; 4AP, 4-aminopyridine; I_{K4AP}, 4-aminopyridine-induced K^+ currents; PZ, pirenzepine; Meth, methoctramine; 4-DAMP, 4-diphenylacetoxy-*N*-methylpiperidine methiodide; *p*-F-HHSiD, hexahydro-sila-difenidol hydrochloride, *p*-fluoro analog; Trop, tropicamide; [^{3}H]NMS, [*methyl*-^{3}H]*N*-scopolamine methyl chloride; pK_i, equilibrium dissociation constant; RT, reverse transcription; PCR, polymerase chain reaction; I_{Kr}, rapid component of delayed rectifier K^+ current; I_{Ks} slow component of delayed rectifier K^+ current.

studies have provided data showing the expression of other subtypes in cardiac tissues as well. For example, mRNAs coding for M_2, M_3, and M_4 isoforms have been shown to express in the chick heart (Tietje et al., 1990; Tietje and Nathanson, 1991; Gadbut and Galper, 1994; McKinnon and Nathanson, 1995). Sharma et al. (1996) identified and characterized the M_1 receptors in the rat hearts. Functional data suggesting the presence of novel subtypes of mAChRs in cardiomyocytes have also been reported. For example, Fermini and Nattel (1994) first described a novel delayed rectifier-like K^+ current activated by choline via the stimulation of mAChRs in canine atrial myocytes. Subsequently, Navarro-Polanco and Sànchez-Chapula (1997) demonstrated that 4-aminopyridine (4AP), a K^+ channel blocker, was also able to activate a similar K^+ current in cat atrial cells, an effect requiring the stimulation of mAChRs. Because these currents possess biophysical properties distinct from I_{KACh}, novel subtypes of mAChRs other than M_2 were proposed by the authors as a mechanism underlying the activation of these channels. On the other hand, tetramethylammonium (TMA), a frequently used substance for replacing sodium ions in patch-clamp studies, has been demonstrated to be able to slow heart rate and weaken contractility via stimulation of mAChR in rat hearts (Kennedy et al., 1995). Workers from our laboratory and others have recently suggested that TMA, like 4AP, is also able to induce K^+ currents by interacting with mAChRs (Navarro-Polanco and Sànchez-Chapula, 1998). However, it remains unclear which subtype of mAChRs mediates the actions of TMA.

Taken together, it is quite conceivable that other mAChR subtypes in addition to M_2 also may exist in the heart. To date, however, little evidence has been submitted concerning the character and functionality of these subtypes in the heart. The goal of the present study was to explore mAChR subtypes in the canine heart using TMA and 4AP as pharmacological probes.

Materials and Methods

Cell Isolation. Single canine atrial myocytes were isolated according to previously described techniques (Yue et al., 1997). The right atrium from adult mongrel dogs (20–26 kg) of either sex was quickly dissected and mounted via the right coronary artery to a Langendorf perfusion system. The preparation was perfused with Ca^{2+}-containing Tyrode's solution at 37°C until the effluent was clear of blood and then switched to Ca^{2+}-free Tyrode's solution for 20 min at a constant rate of 12 ml/min, followed by perfusion with the same solution containing collagenase (110 U/ml CLS II collagenase; Worthington Biochemical, Freehold, NJ) and 0.1% BSA (Sigma Chemical Co., St. Louis, MO). The dispersed cells were stored in KB medium at 4°C for later electrophysiological experiments.

Solutions and Drugs. The Tyrode's solution for cell isolation and whole-cell patch-clamp recording was composed of 136 mM NaCl, 5.4 mM KCl, 1 mM $MgCl_2$, 0.33 mM NaH_2PO_4, 5 mM HEPES, 10 mM glucose, and 1 mM $CaCl_2$, pH adjusted to 7.4 with NaOH. The KB medium for cell storage contained 20 mM KCl, 10 mM KH_2PO_4, 25 mM glucose, 70 mM potassium glutamate, 10 mM β-hydroxybutyric acid, 20 mM taurine, 10 mM EGTA, 0.1% albumin, and 40 mM mannitol, pH adjusted to 7.4 with KOH. The pipette solution contained 0.1 mM GTP, 110 mM potassium aspartate, 20 mM KCl, 1 mM $MgCl_2$, 5 mM Mg-ATP, 10 mM HEPES, 10 mM EGTA, and 5 mM phosphocreatine, pH adjusted to 7.3 with KOH. Contamination by sodium current was prevented by holding the cells at −50 mV. Potential contamination by other currents was minimized by including the following compounds in the bath solution: 1 μM dofetilide (to inhibit I_{Kr}), 20 μM 293B (to block I_{Ks}), 10 μM glyburide (to prevent ATP-sensitive K^+ current), and 200 μM Cd^{2+} (to suppress calcium current). All chemicals were purchased from Sigma Chemical Co., except for 293B, which was a kind gift from Hoechst Pharmaceuticals (Frankfurt, Germany).

Patch-Clamp Techniques. Patch-clamp recording techniques used in this study have been described in detail elsewhere (Wang et al., 1994). Ionic currents were recorded with the whole-cell voltage-clamp methods using an Axopatch 200B amplifier (Axon Instruments, Burlingame, CA). Borosilicate glass electrodes (1 mm A) had tip resistances of 1 to 3 MΩ when filled with pipette solution. Junction potentials were zeroed before formation of the membrane-pipette seal in Tyrode's solution. Mean seal resistance averaged 15 ± 1 GΩ. Several minutes after seal formation, the membrane was ruptured by gentle suction to establish the whole-cell configuration. The capacitance and series resistance (*Rs*) was electrically compensated to minimize the duration of the capacitative surge on the current recording and the voltage drop across the clamped cell membrane. *Rs* along the clamp circuit was estimated by dividing the time constant obtained by fitting the decay of the capacitative transient by the calculated membrane capacitance (the time integral of the capacitative response to a 5-mV hyperpolarizing step from a holding potential of 0 mV divided by the voltage drop). Before *Rs* compensation, the decay of the capacitative surge was a single exponential function of time with a time constant of 412 ± 21 ms (cell capacitance, 82 ± 5 pF; $n = 54$ cells). Precompensation *Rs* values averaged 5.0 ± 0.4 MΩ. After compensation, the time constant was reduced to 111 ± 4 ms (cell capacitance, 71 ± 4 pF), and *Rs* was reduced to 1.4 ± 0.1 MΩ. Currents recorded during the present study rarely exceeded 2.0 nA. The mean maximum voltage drop across the *Rs* was thus in the range of 3 mV. Cells with changing leak current (indicated by >10 pA changes in holding current at −50 mV) were rejected. Experiments were conducted at 36 ± 1°C.

Membrane Receptor-Binding Assay. Fresh atrial tissues dissected from canine hearts were minced and washed with ice-cold PBS buffer. The tissues were then homogenized with a Polytron in 15 ml of ice-cold lysis buffer containing 5 mM Tris·HCl and 2 mM EDTA, pH 7.4, plus a protease inhibitor cocktail consisting of 5 μg/ml phenylmethylsulfonyl fluoride, 10 μg/ml benzamidine, and 5 μg/ml soybean trypsin inhibitor. The homogenate was centrifuged at 500*g* for 15 min at 4°C. The pellets were then homogenized as before and spun again, and the supernatants were pooled. The supernatants were centrifuged at 45,000*g* for 15 min, and the pellets (membrane fractions) were washed twice in the same buffer. The membrane fractions were resuspended in a buffer containing 75 mM Tris·HCl, pH 7.4, 12.5 mM $MgCl_2$, and 5 mM EDTA. The protein content was determined with a Bio-Rad Protein Assay kit (Bio-Rad, Mississauga, ON) using BSA as the standard.

Saturation-binding assays were performed using eight concentrations of [*methyl*-^{3}H]*N*-scopolamine methyl chloride ([^{3}H]NMS) ranging from 2 to 2500 pM. Nonspecific binding was measured in the presence of 1 μM atropine. Experiments were carried out in triplicate for each experiment with total of four individual preparations. Incubations (90 min at room temperature) were terminated by rapid filtration using GF/B filters (Xymotech, Montreal, PQ), and radioactivity was counted with an LS6500 Scintillation Counter (Beckman, Fullerton, CA) with average efficiency of 58%.

Competition-binding assays were carried out as follows. Homogenates were incubated with 400 pM [^{3}H]NMS with pirenzepine (PZ; 0.3 nM to 100 μM), methoctramine (Meth; 0.3 nM to 100 μM), 4-diphenylacetoxy-*N*-methylpiperidine methiodide (4-DAMP; 0.1 nM to 100 μM), or tropicamide (Trop; 1 nM to 100 μM), TMA (30 nM to 1 mM), and 4AP (30 nM to 1 mM), respectively. Fixed amounts of membrane protein (100 μg) were used for each sample in the binding study. Six individual experiments were performed with each determination performed in duplicate for each compound. Chemicals and

reagents for the binding study were purchased from Research Biochemicals International (Natick, MA)

Reverse Transcription-Polymerase Chain Reaction. RNA isolation and reverse transcription-polymerase chain reaction (RT-PCR) methods were the same as previously described (Wang et al., 1996, 1997, 1998). The total RNA samples extracted from canine atrial tissues were incubated with DNase I (0.1 U/μl) at 37°C for 15 min, followed by phenol/chloroform extraction to remove the genomic DNA. Integrity of total RNA was evaluated by ethidium bromide staining in denaturing agarose gels. RT was carried out in a 20-μl reaction mixture containing 1× reaction buffer (10 mM Tris·HCl, pH 8.3, 50 mM KCl, 2.5 mM $MgCl_2$), 1 mM concentrations of dNTPs (Boehringer Mannheim, Montreal, Quebec, Canada), 3.2 μg of random primers $p(dN)_6$ (Boehringer Mannheim), 5 mM dithiothreitol, 50 U of RNase inhibitor (Gibco BRL, Ontario, Canada), and 200 U of Moloney murine leukemia virus reverse transcriptase (Gibco BRL). First-strand cDNAs were synthesized at 42°C for 60 min, and the remaining enzymes were inactivated by heating at 99°C for 5 min. First-strand cDNA (5 μl) resulting from RT was used as a template for amplification in a 25-μl reaction mixture. Reagents included in each reaction contained 10 mM Tris·HCl, pH 8.3, 50 mM KCl, 1.5 mM $MgCl_2$, 1 mM concentrations of dNTPs, 0.5 μM concentration of each gene-specific primer, and 2.5 U of *Taq* polymerase (Gibco BRL). Reactions were hot-started at 94°C and continued for 3 min of initial melting. The cycling profiles were 30 s of denaturing at 94°C, 30 s of annealing at 50°C, and 40 s of extension at 72°C, for 30 cycles, followed by a final extension step of 5 min at 72°C.

The primers used in this study were for m_1 isoform, gggtggcagcagcagcagc (sense) and ctcctttccacggggcttctg (antisense); for m_2 isoform, aagaaggacaagaaggagcc (sense) and ctttggaatggcccagg (antisense); for m_3 isoform, tgcaggcccagaagagc (sense) and ccttttccgcttagtgatctg (antisense); and for m_4 isoform, cccgaaggagaagaaagc (sense) and agtggtggcctctgtgg (antisense). They were synthesized by Gibco BRL. Because the canine cDNA sequences for mAChRs were not available, cloning of fragments was required. For this purpose, degenerate primers for varying isoforms of mAChRs were designed based on published sequences, and unique oligonucleotide sequences were chosen from cDNA regions bearing minimal homology among the different mAChR subtypes and minimal heterogeneity among the species for a given subtype. RT-PCR was used first to obtain the cDNA fragments from RNA extracts of canine right atrium. PCR products were size-separated on 1.5% agarose gels. Bands of desired size were purified with the Glassmax DNA Isolation Spin Cartridge System (Gibco BRL). The purified DNA fragments were subcloned into pGEM-T easy vector (Promega, Madison, WI). Sequences of all constructs were analyzed with Sequenase V2.0 (Amersham Life Science, Cleveland, OH). Gene-specific primer pairs were designed based on our cloned canine cDNA sequences. No sequences matching m_1 receptor cDNA could be obtained from dog hearts. Therefore, primers used for m_1 was designed from human sequence. All primers were designed to avoid significant secondary and complementary structures with about 50 to 60% G-C contents. Specificity of the primer pairs was verified by comparison with entire GenBank database using BLAST and FASTA and by amplification of a PCR product of the predicted size visible as a discrete single band with ethidium bromide staining on agarose gel.

To ensure that the RNA samples used in our experiments were free of contamination with RNA from sources other than cardiac tissue such as neurons or vascular cells, additional experiments were conducted and the detailed description is provided in *Results*.

Data Analysis. Group data are expressed as mean ± S.E. Statistical comparisons were performed on raw data with Student's *t* test, with a two-tailed $p < .05$ taken to indicate a statistically significant difference. Binding data were analyzed using curve-fitting functions of the Prism software (GraphPAD Software, La Jolla, CA). To ensure validity and accuracy of displacement-binding studies, linear regression was performed on the percent bound versus the ratio of bound over free ligand and only data with a regression coefficient of 0.9 were accepted for analyses. The *F* test was used to compare fits for the competition-binding data, and the best fit (one-site binding versus two-site binding) was determined by the probability value for the *F* test and by the change in the residual sum of squares for the two different fits. One- and two-site models were tested for all data sets, and the model yielding the least residual sum of squares was taken to describe the data.

Results

As illustrated in Fig. 1A, the currents conducting either outward or inward currents in response to depolarizing or hyperpolarizing voltage steps in the presence of TMA were consistently observed (middle and were not seen before exposure of the cells to TMA (left). TMA-induced outward currents were characteristic of delayed rectifier K^+ currents with slow time-dependent activation to a peak during depolarization and deactivation tail currents on repolarization to −30 mV. The effects of TMA were concentration-dependent (1 μM to 10 mM), with detectable induction of the currents at a concentration of as low as 1 μM and significant ($p < .05$, compared with baseline recordings) induction of the currents at 10 μM. Maximal level of the current induction was reached at a concentration of 0.5 mM. Hence, 0.5 mM TMA was used in the remainder of the experiments.

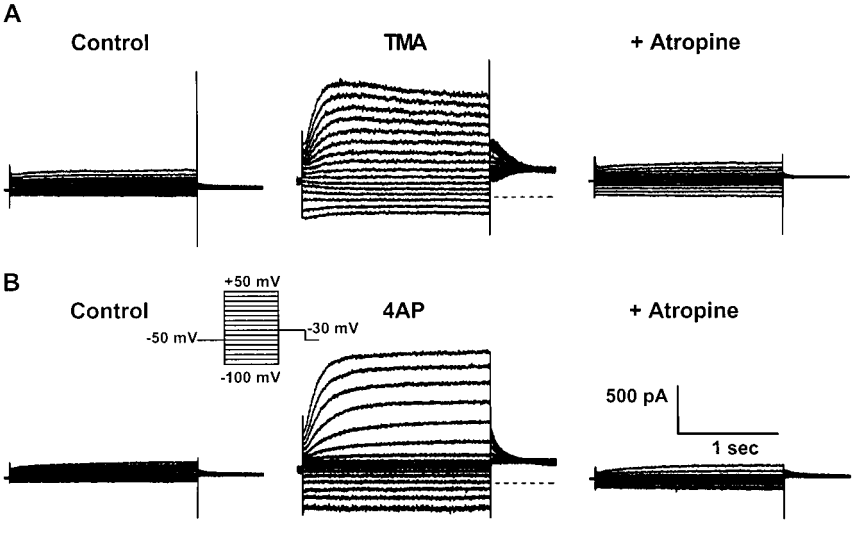

Fig. 1. Activation of novel K^+ currents by TMA and 4AP via simulation of mAChRs in canine atrial myocytes. Currents were elicited by 2-s pulses to potentials ranging from −100 to +50 mV with 10-mV increment followed by a 1-s step to −30 mV. Voltage steps were delivered from a holding potential (HP) of −50 mV at an interpulse interval of 5 s. A, raw current traces obtained from a representative myocyte, showing the baseline recordings before TMA application (left), currents activated in the presence of TMA (0.5 mM, I_{KTMA}, middle), and elimination of the currents by atropine (1 μM) applied to the bath containing TMA (right). B, typical examples of 4AP-induced currents recorded from a representative cell. Left, the baseline recordings before 4AP application, currents induced in the presence of 4AP (1 mM, I_{K4AP}; middle), and abolishment of the currents by atropine (1 μM) applied to the solution containing 4AP (right). Dashed line indicates a zero current level.

Similar to TMA, bath application of 4AP (1 mM) also consistently led to activation of voltage-dependent currents similar to TMA-induced currents with conductance in both outward (depolarizing pulses) and inward (hyperpolarizing pulses) directions. Representative current traces are shown in Fig. 1B. The size of 4AP-induced currents also depended on 4AP concentration (50 μM to 2 mM), with maximal effects occurring at a concentration of 1 mM. Thus, 1 mM 4AP was used to study the 4AP-induced currents in the remainder of our experiments. There was no apparent run-down of TMA- or 4AP-induced currents under our experimental conditions with stable whole-cell recordings up to 2 h. In both cases, the current induction was seen right after (within 3 min) the wash-in of the drugs into the bath.

Both currents reversed at around the K^+ equilibrium potential (−80 mV) according to Nernst equation under our experimental conditions (−73.4 ± 5.6 mV for TMA-induced currents, $n = 3$; and −70.2 ± 7.2 mV for 4AP-induced currents, $n = 3$). Furthermore, the reversal potentials of both TMA- and 4AP-induced currents, as determined by the tail currents elicited at various potentials ranging from −120 to −30 mV, became less negative with elevating concentrations of external K^+ (isotonic replacement of Na^+ with K^+ from 5.4 to 10.8 and 130 mM, respectively). The calculated slope factor from linear regression of reversal potentials (as a function $[K^+]_o$) were 51.3 ± 3.3 and 50.2 ± 5.2 mV/decade for TMA- and 4AP-induced currents, respectively, suggesting that both currents were predominantly carried by K^+.

To investigate whether the currents were resulted from TMA/4AP modulation of known K^+ currents, we evaluated the effects of varying K^+ channel blockers on TMA- and 4AP-induced K^+ currents. These blockers included glyburide (10 μM for I_{KATP}), dofetilide (1 μM for I_{Kr}), indapamide (100 μM for I_{Ks}), 293B (20 μM for I_{Ks}), and Cd^{2+} (200 mM for I_{Ca}). We failed to observe any significant alterations of TMA- and 4AP-induced currents in the presence of any one of these compounds, suggesting that these two currents are distinct from the known potassium currents previously found in the heart. We therefore included glyburide, dofetilide, 293B, and Cd^{2+} in the perfusate for the remainder of our experiments. For the sake of convenience, we used abbreviated labels I_{KTMA} and I_{K4AP} to describe the TMA- and 4AP-induced K^+ currents, respectively, in the remainder of the article.

The above data indicated that I_{KTMA} and I_{K4AP} probably represent novel currents similar to recently described K^+ currents in dog atrium (Fermini and Nattel, 1994) and cat atrium (Navarro-Polanco and Sànchez-Chapula, 1997), respectively, for which the activation of mAChRs was required. Indeed, atropine (1 μM), a nonselective mAChR antagonist, quickly abolished I_{KTMA} and I_{K4AP}. The results are displayed in Fig. 1 (right). Similar results were observed in total of 11 cells for I_{KTMA} and 10 cells for I_{K4AP}.

The atropine data indicate that stimulation of mAChRs is required for the activation of I_{KTMA} and I_{K4AP}. It is known, however, that an M_2 receptor is the only mAChR subtype functionally identified in cardiac cells (Yatani et al., 1988; Takano and Noma, 1997) and that stimulation of an M_2 receptor by ACh or carbachol induces an inward rectifier K^+ current, I_{KACh}. If it is true that only M_2 receptors exist in the heart, then why would TMA- or 4AP-induced current demonstrate delayed rectifying properties distinct from I_{KACh}? One of the possible explanations for this apparent contradiction is that there are other subtypes of mAChRs in addition to M_2 receptors in canine atrial myocytes, which mediate the activation of I_{KTMA} and I_{K4AP}. We therefore explored the possible role of mAChR subtypes in canine atrial myocytes. We first carried out experiments to evaluate the effects of pertussis toxin (PTX) on I_{KTMA} and I_{K4AP}. PTX was applied intracellularly through the dialysis of pipette solution containing 2 μg/ml PTX. Currents were recorded immediately after membrane rupture and taken as baseline values. Then, same recordings were repeated every 5 min, and currents recorded 20 min after membrane rupture were used for data analysis representing steady-state effects of PTX because 10 min was sufficient to allow the complete dialysis of PTX into the cellular plasma under our experimental conditions. No significant changes ($p > .05$, compared with baseline values, $n = 5$ cells) in I_{KTMA} were observed in the presence of PTX (Fig. 2A). In sharp contrast, I_{K4AP} was nearly abolished ($p < .05$, $n = 5$) by PTX, as shown in Fig. 2C. For comparison, the effects of PTX on I_{KACh} were also determined, and similar results to those seen with I_{K4AP} were observed. As mentioned, neither I_{KTMA} nor I_{K4AP} demonstrated any rundown during the recording. This validates our PTX experiments described above. To further confirm the observations, the effects of extracellularly applied PTX on I_{KTMA} and I_{K4AP}

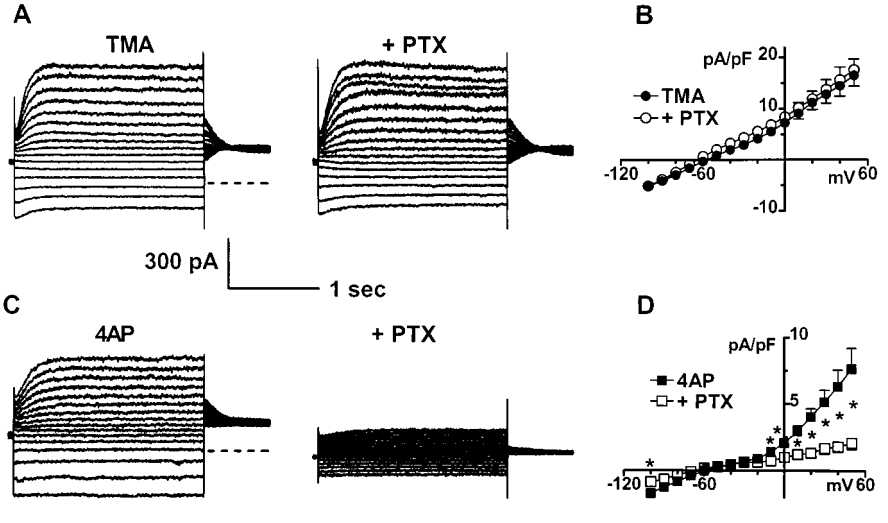

Fig. 2. Effects of PTX, a G_i/G_o protein inhibitor, on I_{KTMA} and I_{K4AP} in canine atrial myocytes. PTX (2 μg/μl) was applied intracellularly by dialysis through the pipette solution. A, analog data shows I_{KTMA} traces recorded immediately after membrane rupture (left) and 20 min after membrane rupture (middle) in the presence of TMA. Right, current density-voltage relation of I_{KTMA} averaged from five cells. B, current density-voltage relationship of I_{KTMA} before and after PTX treatment (averaged data from a total of five cells tested). C, effects of PTX on I_{K4AP}. Shown is a family of current traces recorded in the presence of 4AP immediately after membrane rupture (left) and 20 min after membrane rupture (middle). D, current density-voltage relationship of I_{K4AP} before and after PTX treatment ($n = 5$). Dashed line indicates a zero current level. *$p < .05$ comparison between before and after PTX.

were also assessed. In these experiments, cells were divided into two groups: the control group and the PTX group. The cells of the PTX group were preincubated with a final concentration of 5 μg/ml PTX in KB solution at 36°C for 90 min. The control cells were subjected to the same procedure but without PTX in the solution. Then, patch-clamp recording was carried out to study the inducibility of I_{KTMA} or I_{K4AP} in cells from the PTX group compared with cells from the control group. Consistent with the results from intracellular application of PTX, pretreatment with PTX did not alter TMA (0.5 mM) induction of I_{KTMA} compared with the control cells. For example, the I_{KTMA} density, measured at +50 mV, was 9.8 ± 1.3 pA/pF for the control group (n = 8) and 9.6 ± 0.8 pA/pF for the PTX group (n = 7, $p > .05$). In contrast, the ability of 4AP to induce I_{K4AP} was completely paralyzed by PTX. The current density of I_{K4AP} was 6.3 ± 0.6 pA/pF (n = 3) for the control cells, and this value was decreased to 0.1 ± 0.0 pA/pF (n = 3, $p < .01$) with the PTX-pretreated cells.

The results of the PTX experiments suggest that I_{KTMA} is probably mediated by an M_1, M_3, or M_5 receptor subtype because these subtypes are characterized biochemically by coupling to inositol phosphate production via a PTX-insensitive G protein (Peralta et al., 1988), whereas I_{K4AP} is likely mediated by M_2 or M_4 subtype because the transduction machinery for these subtypes has been shown to be PTX sensitive (Peralta et al., 1988). To further pinpoint the mAChR subtype specificity of I_{KTMA} and I_{K4AP}, we explored the relationship between the currents and the receptor subtypes by using pharmacological probes selective to different mAChR subtypes. No appreciable alterations in I_{KTMA} were found after the application with PZ (an M_1-selective antagonist; 10 nM) (Watson et al., 1983; van Zwieten and Doods, 1995), Meth (an M_2-selective antagonist; 20 nM) (Michel and Whiting, 1988; van Zwieten and Doods, 1995), or Trop (an M_4-selective antagonist; 200 nM) (Lazareno et al. 1990; Lazareno and Birdsall, 1993). No attempt was made to study the effects of higher concentrations of these compounds because subtype specificity is lost at higher concentrations. 4-DAMP, an M_3-selective antagonist (Barlow and Shepherd, 1986; Michel et al., 1989; Araujo et al., 1991; van Zwieten and Doods, 1995), produced concentration-dependent suppression of I_{KTMA}. As shown in Fig. 3, the currents were reduced by approximately 50% at a concentration as low as 2 nM for both depolarization- and hyperpolarization-induced currents (Table 1), and complete inhibition was achieved with 10 nM 4-DAMP. In the case of I_{K4AP}, as shown in Fig. 4, only the M_4 inhibitor Trop caused significant depression of the current amplitude without changing the kinetics. The current density at +50 mV was reduced 46 ± 3% by 200 nM, 68 ± 5% by 1 μM, and 93 ± 8% by 10 μM Trop (n = 5 for each). Other compounds, like PZ (10 nM), Meth (20 nM), and 4-DAMP (2 nM), failed to alter I_{K4AP}.

Our data suggest that I_{KTMA} might be mediated by M_3 receptors and that I_{K4AP} might be mediated by M_4 receptors. To acquire more conclusive evidence, we assessed the effects of 4-DAMP and Trop on the concentration-dependent responses to TMA (1 μM to 2 mM) and 4AP (10 μM to 2 mM), respectively. The current density obtained at +50 mV was used to determine the drug effects. As shown in Fig. 5A, 4-DAMP (2 nM) caused a parallel shift of the concentration-response curve of I_{KTMA} to the right. The EC_{50} value of TMA was 129 μM with a Hill coefficient of 2.3 in the absence of 4-DAMP and 447 μM ($P < .05$, n = 3) with a Hill coefficient of 1.7 in the presence of 4-DAMP. Similar effects of Trop on I_{K4AP} were observed (Fig. 5B). The EC_{50} value of 4AP for I_{K4AP} induction was 181 μM for 4AP alone versus 391 μM ($P < .05$, n = 3) for 4AP in the presence of Trop (200 nM). The calculated Hill coefficient was 1.3 for both with and without Trop.

We also tested the ability of two other M_3-selective inhibitors: 4-DAMP mustard (an irreversible M_3 antagonist; 4 nM, n = 5) (Ehlert and Griffin, 1988) and hexahydro-sila-difenidol hydrochloride, p-fluoro analog (p-F-HHSiD; 20 nM, n = 5) (Lambrecht et al., 1988), to suppress I_{KTMA}. We observed 49.4 ± 3.3% reduction in current at +50 mV by 4-DAMP mustard ($p < .01$, n = 3) and 56 ± 8% reduction in current by p-F-HHSiD ($p < .05$, n = 3). It is generally agreed that the use of an irreversible receptor inactivation plus concurrent receptor protection can enhance selective alkylation (Ehlert and Griffin, 1988; Eglen et al., 1994). In our experiments, we first incubated the cells with antagonists for $M_1/M_2/M_4$ subtypes to protect these receptors, if any, and

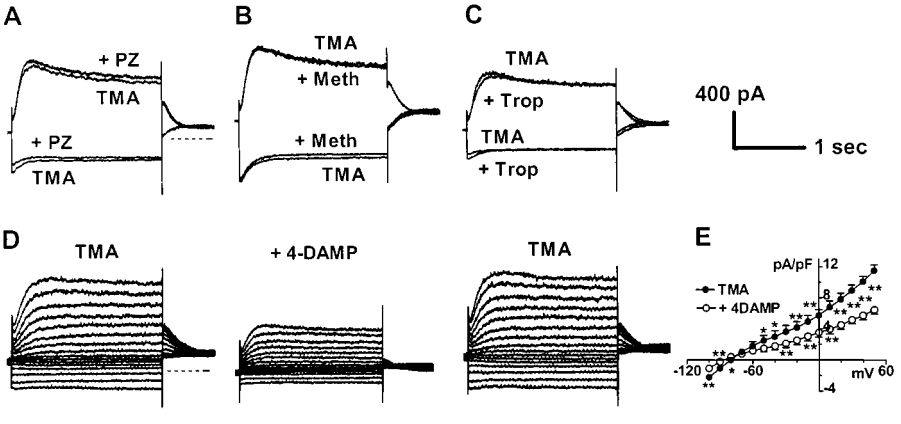

Fig. 3. Effects of mAChR subtype-selective antagonists on I_{KTMA} in canine atrial myocytes. Currents were elicited in the presence of 0.5 mM TMA, with voltage protocols same as described in Fig. 1. A, effects of M_1-selective antagonist PZ (10 nM). Raw current traces before and after PZ are superimposed, and only currents recorded at +50 mV and −100 mV are shown for the sake of clarity. B, effects of M_2-selective antagonist Meth (20 nM). C, effects of M_4-selective antagonist Trop (200 nM). D, representative experiments showing the effects of M_3-selective antagonist 4-DAMP on TMA-induced K^+ currents. Left, currents before wash-in of 4-DAMP. Middle, currents in the presence of 4-DAMP (2 nM). Right, currents after washout of 4-DAMP. E, current density-voltage relationship of baseline current and after exposure of cells to 4-DAMP at a concentration of 2 nM. Dashed line indicates a zero current level. *$p < .05$ and **$p < .01$, comparison between before and after 4-DAMP (n = 6).

then applied alkylating agent 4-DAMP mustard to inactivate the unprotected subtype (i.e., M_3 receptors). The same degree of I_{KTMA} suppression by 4-DAMP mustard was seen with and without protection, strongly suggesting the role of M_3 subtype in canine myocytes.

It is known that M_2 subtype mediates ACh-induced inward rectifier K^+ current (I_{KACh}) in cardiac cells. Consistent with this notion, none of the antagonists except for Meth, an M_2-selective inhibitor, had any detectable effects on I_{KACh} at concentrations tested in our experiments (Fig. 6). By comparison, Meth at 20 nM substantially diminished I_{KACh} (Table 1). Meth (20 nM) did not alter the concentration-response curves of I_{KTMA} and I_{K4AP} (Fig. 5), suggesting a minimal contribution of M_2 to these currents. An immediate question that one might ask is whether ACh, as a nonselective mAChR agonist, could also activate I_{KTMA} and I_{K4AP}. As shown in Fig. 6D, when Meth was added to the ACh-containing solution, I_{KACh} was reduced due to inhibition of M_2 receptors. Meanwhile, there was an increase in the outward currents. The outward portion of I_{KACh} without Meth had strong inward rectification, but in the presence of Meth, the outward currents displayed outward rectification, and this is clearly seen with the current-voltage curves shown in Fig. 6E. To determine whether these outward currents were the results of activation of M_3/M_4 receptors by ACh unmasked when M_2 receptors were largely inhibited, we evaluated the effects of

TABLE 1
Effects of mAChR subtype-selective antagonists on I_{KTMA}, I_{K4AP}, and I_{KACh}

		Pirenzepine, 10 nM	Methoctramine, 20 nM	4-DAMP, 2 nM	Tropicamide, 200 nM
			pA/pF		
I_{KTMA}					
+50 mV	Control	13.9 ± 2.1	12.7 ± 2.7	11.5 ± 0.6	9.0 ± 1.1
	Drug	14.0 ± 2.0	12.2 ± 2.7	6.4 ± 0.4**	9.1 ± 1.2
	% change	1.0 ± 3.5	−4.0 ± 0.6	−42.8 ± 6.1	0.5 ± 1.7
−100 mV	Control	4.2 ± 0.9	4.1 ± 1.0	2.2 ± 0.3	3.5 ± 0.8
	Drug	4.3 ± 0.5	4.2 ± 0.9	1.1 ± 0.2**	3.8 ± 1.0
	% change	5.8 ± 8.2	3.1 ± 4.0	−50.9 ± 5.1	5.2 ± 7.4
		(*n* = 4)	(*n* = 5)	(*n* = 6)	(*n* = 4)
I_{K4AP}					
+50 mV	Control	6.8 ± 1.5	7.8 ± 0.9	8.7 ± 0.2	7.1 ± 1.0
	Drug	6.9 ± 1.6	8.0 ± 0.8	9.0 ± 0.5	3.8 ± 0.5**
	% change	1.5 ± 3.8	−3.7 ± 0.9	7.2 ± 3.4	−46.4 ± 3.1
−100 mV	Control	3.8 ± 1.1	3.4 ± 1.0	3.8 ± 1.5	2.7 ± 0.3
	Drug	4.1 ± 1.2	3.8 ± 1.6	3.7 ± 1.3	1.6 ± 0.2***
	% change	5.9 ± 3.0	12.9 ± 4.4	−0.7 ± 5.1	−41.8 ± 4.5
		(*n* = 3)	(*n* = 3)	(*n* = 4)	(*n* = 5)
I_{KACh}					
+50 mV	Control	7.0 ± 1.0	6.4 ± 0.6	5.9 ± 0.9	6.2 ± 0.5
	Drug	6.9 ± 1.2	9.4 ± 1.0**	5.7 ± 0.5	6.1 ± 0.3
	% change	−0.2 ± 0.3	44.8 ± 4.0	−3.4 ± 0.5	−1.6 ± 1.0
−100 mV	Control	11.2 ± 3.0	9.4 ± 2.1	10.4 ± 1.3	9.1 ± 1.8
	Drug	10.9 ± 4.1	14.8 ± 1.1	9.8 ± 3.5	8.9 ± 2.1
	% change	−1.0 ± 0.4	−57.4 ± 4.7***	−5.2 ± 1.2	−2.2 ± 2.2
		(*n* = 3)	(*n* = 6)	(*n* = 3)	(*n* = 3)

* p < .05, ** p < .01, *** p < .001. Student's *t* test, compared with control.

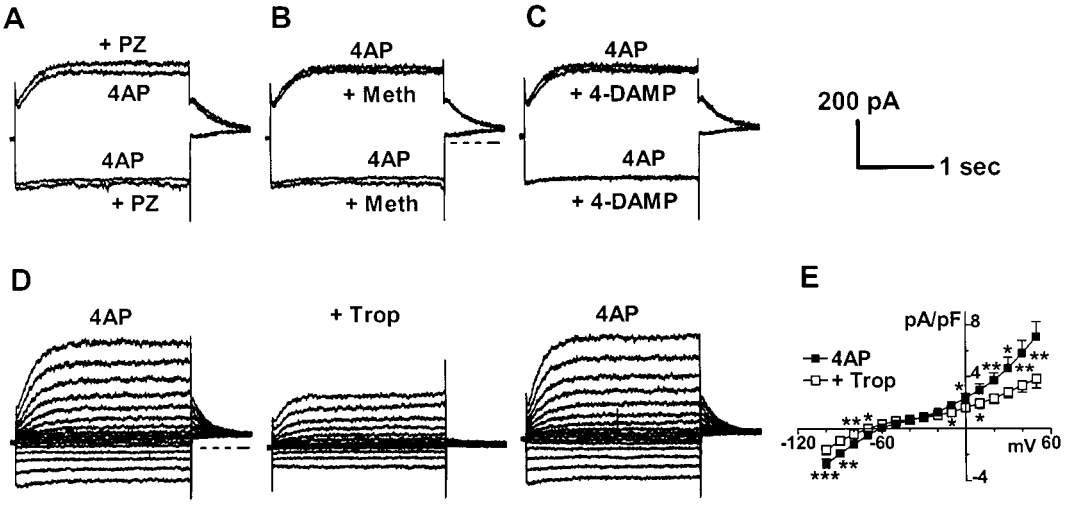

Fig. 4. Effects of mAChR subtype-selective antagonists on I_{K4AP} in canine atrial myocytes. Currents were elicited in the presence of 1 mM 4AP. A through C, effects of PZ (10 nM), Meth (20 nM), and 4-DAMP (2 nM) on I_{K4AP}, respectively. Raw current traces before and after the drugs are superimposed, and only currents recorded at +50 mV and −100 mV are shown for the sake of clarity. D, representative experiments showing the effects of M_4-selective antagonist Trop on I_{K4AP}. Left, currents before wash-in of Trop. Middle, currents in the presence of Trop (200 nM). Right, currents after washout of Trop. E, current density-voltage relationship of baseline current and after exposure of cells to Trop at a concentration of 200 nM. Dashed line indicates a zero current level. *$p < .05$, **$p < .01$, and ***$p < .01$, comparison between before and after Trop.

4-DAMP or Trop on these outward currents. The results from representative experiments are illustrated in Fig. 7. Our data demonstrated that both 4-DAMP (2 nM) and Trop (200 nM) were able to depress the currents and the 4-DAMP- or Trop-sensitive currents, obtained by digital subtraction between the currents with and without 4-DAMP or Trop, had waveforms similar to I_{KTMA} or I_{K4AP}, suggesting that M_3 and M_4 receptors were involved in the activation of ACh-induced outward currents in the presence of Meth. The extents of block by 4-DAMP or Trop varied greatly, presumably depending on the relative amount of M_3 or M_4 receptors activated in each individual cell. It should be emphasized that the outward currents induced by ACh in the presence of Meth were observed only from 16 of 29 cells studied. To investigate whether the outward currents induced by ACh were actually due to nonspecific or some unknown effects of Meth, we applied Meth (20 nM) alone to the bath. Meth itself failed to induce any kinds of ion currents (Fig. 7C). Furthermore, when the cells were preincubated with 4-DAMP and Trop to prevent the stimulation of M_3 and M_4 receptors, ACh failed to induced the outward currents even after addition of Meth to the solution (Fig. 7D).

Existence of M_3 and M_4 Receptors in Cardiac Cells Demonstrated by Binding Assay. mAChR subtypes demonstrate characteristic affinities for the binding of different muscarinic antagonists. To verify the presence of M_3 and M_4 receptor proteins in cardiac cells, we performed membrane receptor-binding assays. The results are summarized in Fig. 8 and Table 2. Saturation binding of [^{3}H]NMS to the membrane homogenates from canine atria yielded a maximum binding value or mAChR density of 282 ± 26 fmol/mg protein and a dissociation constant K_d of 223 ± 24 pM. Displacement binding of [^{3}H]NMS in the presence of PZ, Meth, 4-DAMP, or Trop was analyzed with a two-site binding model. The pK_i values from competition-binding experiments are listed in Table 2. Note that the K_d values for high-affinity bindings of various antagonists were all closely relevant to the concentrations at which these compounds produced half-maximal inhibition to the currents. For example, the K_d value of 4-DAMP was 2.4 nM, and 2 nM 4-DAMP suppressed about 50% of I_{KTMA}. In addition, the K_d value of Trop binding and the concentration of Trop that caused 50% reduction of I_{K4AP} were 230 and 200 nM, respectively.

If, as our functional study suggested, TMA and 4AP activated I_{KTMA} and I_{K4AP} via stimulation of M_3 and M_4 receptors, respectively, then these two compounds should also be able to displace [^{3}H]NMS binding in a competitive fashion. Indeed, the competition-binding assay performed with TMA and 4AP yielded displacement curves best described with a two-site binding model. The data are shown in Fig. 8C. The

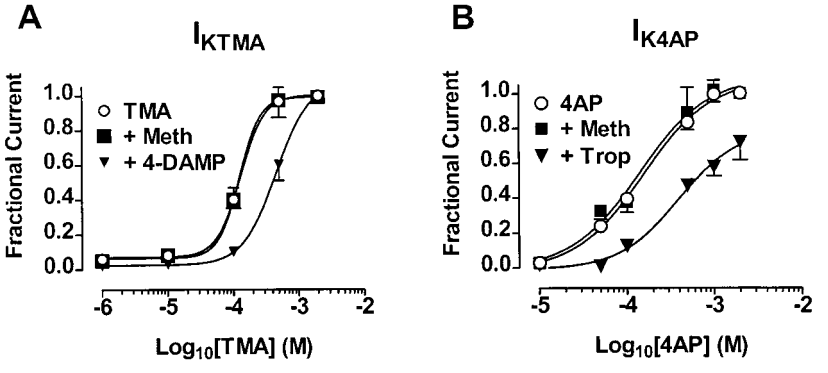

Fig. 5. Effects of mAChR subtype-selective antagonists on the concentration dependence of TMA induction of I_{KTMA} (A) and 4AP-induction I_{K4AP} (B) in canine atrial myocytes. Symbols represent values averaged from three cells, and the lines represent the best fits to the Hill equation: $B/B_{max} = 1/[1 + (EC_{50}/D)^n]$, where B_{max} is the maximum level of currents inducible by agonists (e.g., 2 mM TMA or 2 mM 4AP), B is the current amplitude induced at a drug concentration D, EC_{50} is the concentration of agonists that produces 50% maximum induction of the currents, and n is the Hill coefficient. Note that 4-DAMP (2 nM) or Trop (200 nM) markedly shifts the dose-response curve of I_{KTMA} or I_{K4AP} to the right, but Meth (20 nM) does not alter the concentration dependence of either of the currents.

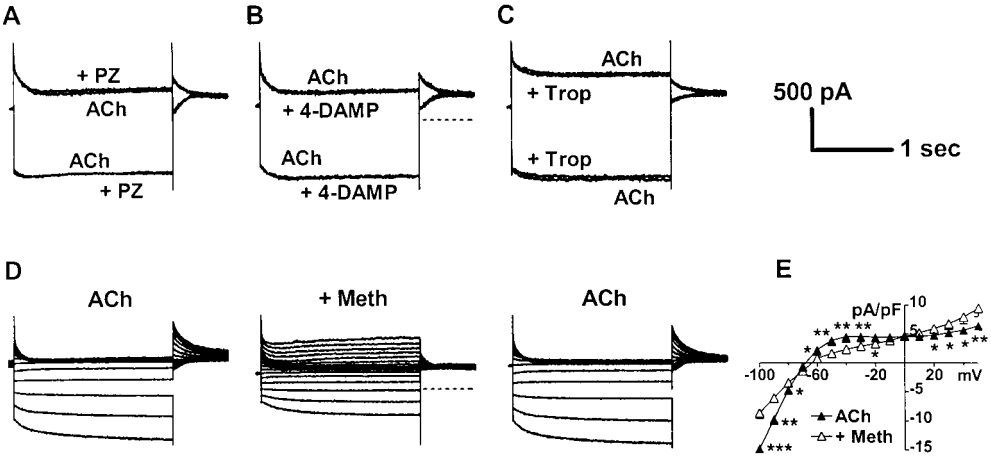

Fig. 6. Effects of mAChR subtype-selective antagonists on I_{KACh} in canine atrial myocytes. Currents were elicited in the presence of 1 μM ACh, with the same voltage protocols as described in Fig. 1. A through C, effects of mAChR subtype-selective antagonists PZ (10 nM), 4-DAMP (2 nM), and Trop (200 nM) on I_{KACh}. Raw current traces before and after the drugs are superimposed, and only recordings obtained at +50 mV and −100 mV are shown. D, representative experiments showing the effects of M_2-selective antagonist Meth (20 nM) on I_{KACh}. Left, currents before wash-in of Meth. Middle, currents in the presence of Meth (20 nM). Right, currents after washout of Meth. E, current density-voltage relationship of baseline current and after exposure of cells to 20 nM Meth. Dashed line indicates a zero current level. *$p < .05$, **$p < .01$, and ***$p < .01$, comparison between before and after Meth.

K_d values were 10.9 μM and 2.5 mM for TMA and 2.5 μM and 0.4 mM for 4AP. These values were both comparable to the concentrations at which these compounds produced induction of I_{KTMA} and I_{K4AP}, respectively.

Expression Profile of mRNA Coding for Various mAChR Isoforms. To obtain further evidence for the presence of multiple subtypes of mAChRs in canine hearts, cloning of cDNA fragments and detection of mRNAs for m_1, m_2, m_3, and m_4 four different isoforms of mAChRs were performed by RT-PCR amplification. We isolated cDNA fragments of 458 bp for m_2, 432 bp for m_3, and 258 bp for m_4 isoforms, but we failed to obtain any sequences matching with m_1 cDNA. These fragments share 91%, 81%, and 80% homology to the same regions of corresponding human m_2, m_3, and m_4 sequences in the amino acid level. These fragments represent parts of the third intracellular loop between transmembrane domains 5 and 6, which is thought to contain critical determinants of G protein-coupling specificity. A representative gel showing the PCR-amplified products representing mRNAs for m_2, m_3, and m_4 subtypes is shown in Fig. 9. The m_2, m_3, and m_4 isoforms were all expressed at significant levels, as indicated by the 297-bp band in lane 4 for m_2, the 216-bp band in lane 6 for m_3, and the 257-bp band in lane 8 for m_4.

Previous investigators have assayed mRNA for the neuronal acetylcholine β4 subunit to exclude neural contamination of cardiac mRNA measurements (Dixon and McKinnon, 1994). We used published sequences of the human nicotinic receptor β4 subunit to design primer pairs for RT-PCR. The β4 subunit mRNA was consistently detected in three samples from rat brain but was absent in dog atrial samples. Contamination by vascular tissue was excluded by RT-PCR amplification of the maxi-K channel (Ca^{2+}-activated K^+ channel). Total RNA isolated from rat vascular smooth muscle, in which maxi-K channels carry a substantial current, was used

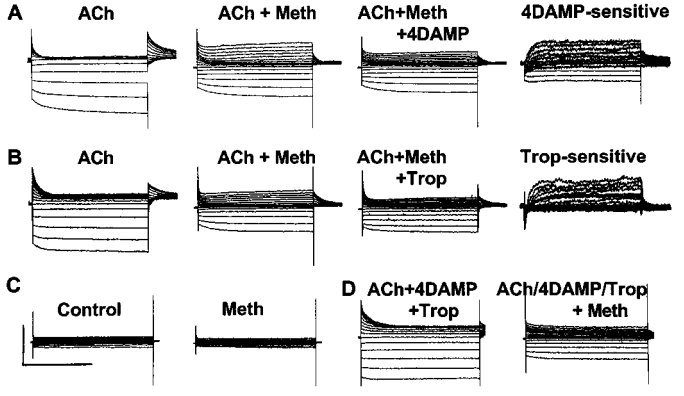

Fig. 7. Effects of 4-DAMP and Trop on the outward currents induced by ACh in the presence of Meth. A, examples showing 4-DAMP (2 nM) blockade of ACh (1 μM)-induced outward currents in the presence of Meth (20 nM) from a representative myocyte. The 4-DAMP-sensitive currents were obtained by digital subtraction of the currents with 4-DAMP from those before 4-DAMP. Similar results were observed in another four cells. B, examples showing Trop (200 nM) blockade of ACh (1 μM)-induced outward currents in the presence of Meth (20 nM) from a representative myocyte. The Trop-sensitive currents were obtained by digital subtraction of the currents in the presence of Trop from those before Trop. Similar data were obtained from a total of five cells. C, experiments demonstrating the failure of Meth (20 nM) alone to induce any currents. The same observations were obtained from all five cells studied. D, experiments showing the inability of ACh to induce the outward current when 4-DAMP (2 nM) and Trop (200 nM) were included in the solution. The addition of Meth still failed to activate the outward current seen in the absence of 4-DAMP and Trop but reduced I_{KACh}. Similar results were acquired from another three myocytes. Horizontal calibration, 1 s. Vertical calibration for all except for the 4-DAMP- and Trop-sensitive currents was 500 pA, and that for the 4-DAMP- and Trop-sensitive currents was 200 pA.

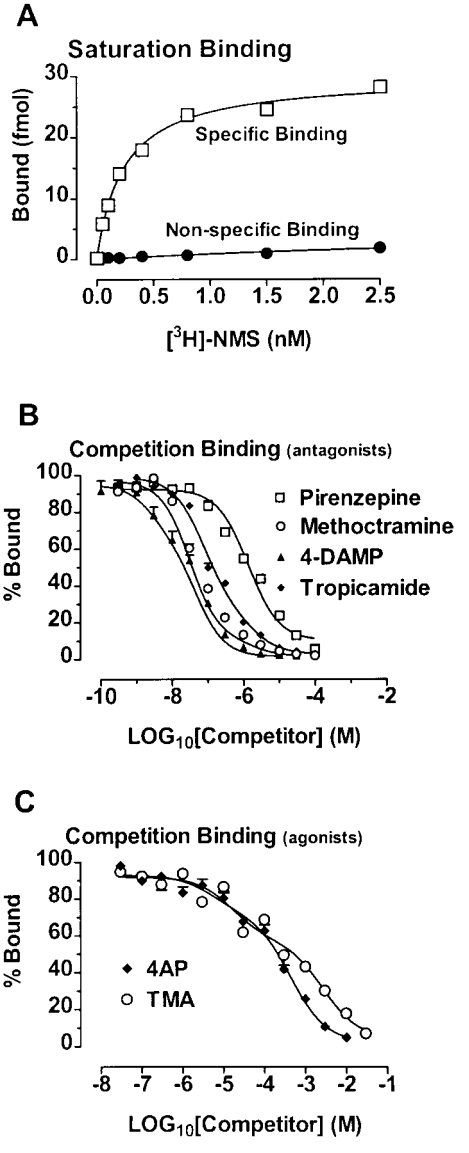

Fig. 8. mAChR binding with [^{3}H]NMS to homogenates of canine atrial tissues. A, saturation binding. Shown are the data averaged from four individual preparations carried out in triplicate for each experiment. Symbols are experimental data and lines represent the fits with a one-site binding model. B, displacement binding of [^{3}H]NMS with varying antagonists. C, displacement binding of [^{3}H]NMS with two agonists: TMA and 4AP. Each point represents the mean ± S.E.M. from six experiments assayed in duplicate. Curves are best fits of the experimental data to a two-site binding model.

TABLE 2

Displacement binding of [^{3}H]NMS by mAChR subtype-selective antagonists and agonists

	K_{i1}	K_{i2}
Pirenzepine	6.9 ± 0.3	5.8 ± 0.2
Methoctramine	7.7 ± 0.6	6.6 ± 0.4
4-DAMP	9.1 ± 0.2	8.1 ± 0.1
Tropicamide	7.6 ± 0.1	6.4 ± 0.2
TMA	5.7 ± 0.2	3.1 ± 0.0
4AP	7.0 ± 0.5	3.9 ± 0.1

as a positive control. PCR primer pairs were designed based on published sequence. Although strong maxi-K channel signal was observed in vascular preparations, no corresponding band was found in dog tissue.

Discussion

One major breakthrough in the field of the cholinergic nervous system is the discovery of multiple subclasses of muscarinic receptors, due to the development of pharmacological probes and molecular cloning techniques. Although M_2 receptors have long been believed to be the only functional mAChR subtype in cardiac cells, our data from functional study (patch-clamp experiments), receptor-binding assays, and mRNA expression detection demonstrate the heterogeneity of mAChRs and their physiological functions in canine atrial cells. There are two major and novel findings in the present study. First, multiple mAChR subtypes (M_2, M_3, and M_4) coexist in canine cardiac cells. Our data represent, to our knowledge, the first to identify and characterize cardiac M_3 and M_4 receptor subtypes in the heart with both functional and binding data. Second, different subtypes of mAChRs are coupled to different K^+ channels in cardiac myocytes.

To date, at least four subtypes of mAChRs have been pharmacologically defined in living systems: M_1, M_2, M_3, and M_4 (Eglen and Whiting, 1990; Mutschler et al., 1995; van Zwieten and Doods, 1995), and five different isoforms of mAChR cDNAs have also been molecularly identified, which are designated as m_1 through m_5 (Bonner et al., 1987; Peralta et al., 1987; Goyal, 1989). It has long been believed that M_2 is the only functional mAChR subtype in cardiac cells (Watson et al., 1983; Bonner et al., 1987; Mizushima et al., 1987; Peralta et al., 1987; Maeda et al., 1988). However, the existence and possible role of M_1 receptors in the rat hearts have been convincingly documented by Sharma et al. (1996). Recent studies with molecular cloning techniques also reported interesting data showing the abundant expression of mRNAs for m_2, m_3, and m_4 subtypes in the chick heart (Tietje et al., 1990; Tietje and Nathanson, 1991; Gadbut and Galper, 1994; McKinnon and Nathanson, 1995). In the present study, we provide three lines of evidence for the coexistence of multiple subtypes of mAChRs in cardiac cell membrane.

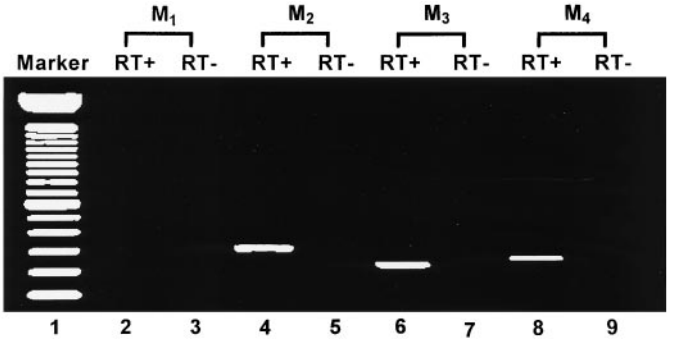

Fig. 9. Detection of mRNAs coding for four isoforms of mAChRs (m_1, m_2, m_3, and m_4) in RNA samples extracted from canine atrium. Shown is a representative gel with ethidium bromide staining of PCR-amplified products. Lane 1, 100-bp cDNA size maker; lanes 2 through 9, expected PCR products for m_1 (338-bp band), m_2 (297-bp band), m_3 (216-bp band), and m_4 (257-bp band), respectively; RT+, reaction with reverse transcriptase; and RT−, omission of reverse transcriptase from the reaction for negative control.

First, our patch-clamp studies, using TMA and 4AP as pharmacological probes and various mAChR subtype-selective antagonists, provide for the first time strong functional evidence for cardiac M_3 and M_4 receptors. The concentrations of antagonists used in our experiments were chosen based on previous studies in the literature and the data from our binding assays, which should provide optimal selectivity to each subtype. For positive control, we also tested the effects of Meth on ACh-induced K^+ current. The fact that Meth (20 nM) indeed inhibited I_{KACh} argued for the validity of concentrations used in our study. On the other hand, the drastic effects of M_3-selective inhibitors could hardly explained by cross-actions on other subtypes of mAChRs because we did not observed any changes in I_{KACh} and I_{K4AP} after the application of M_3 antagonists. Moreover, the significant shifts in concentration-response curves of I_{KTMA} and I_{K4AP} produced specifically by M_3 and M_4 antagonists, respectively, provide more conclusive evidence. The receptor protection-inactivation experiments further strengthen the evidence for the presence of M_3 receptors. The fact that PZ, an M_1-selective antagonist, failed to alter I_{KTMA} and I_{K4AP} rules out the contribution of M_1 receptors to these two currents. The discrepancy between the study of Sharma et al. (1996) and ours likely represents the interspecies difference or tissue type heterogeneity, or both, considering that the rat ventricular cells were used in their study and canine atrial myocytes were used in the present study. The second line of evidence came from our receptor-binding assays of the displacement [^{3}H]NMS binding by various mAChR antagonists. PZ, Meth, 4-DAMP, or Trop yielded pK_i values pointing to the conclusion that there is coexistence of multiple subtypes of mAChRs (M_2/M_3/M_4). The displacement of [^{3}H]NMS binding by PZ yielded a high- and a low-affinity binding site with pK_i values of 6.9 and 5.8, respectively. The high-affinity binding identifies M_3 and M_4 subtypes, and the value for the low-affinity binding is more suggestive of the presence of an M_2 subtype, which is inconsistent with its affinity to an M_1 receptor. Although the high-affinity binding of Meth (pK_i = 7.7) suggests the existence of M_2, M_4, and M_1 subtypes, considering that PZ binding ruled out the possibility of M_1 in canine tissues, it is more likely that Meth actually binds to only M_2 and M_4 receptors (van Zwieten and Doods, 1995). The low-affinity binding of Meth (pK_i = 6.6) identifies but does not distinguish M_3 and M_5 subpopulations. Similarly, 4-DAMP binding revealed two groups of mAChRs, with high-affinity binding (pK_i = 9.1) in agreement with its affinity to M_3 and M_1 receptors and low-affinity binding (pK_i = 7) for an M_2 subtype of mAChRs. However, in respect to PZ binding, the high-affinity pK_i value for 4-DAMP binding would more likely correspond to an M_3 receptor. Competition binding of Trop gave a high-affinity binding site (pK_i = 7.6) that fits well with the existence of an M_4 receptor subtype (Lazareno et al., 1990; Lazareno and Birdsall, 1993). The low-affinity binding of Trop (pK_i = 6.1) does not seem to identify any subtypes of the known mAChRs. Taken together, the results from our binding experiments suggest the coexistence of multiple subtypes, M_2, M_3, M_4, and probably M_5 as well, of mAChRs in the canine atrium. More interestingly, the K_d value from binding assay is almost identical with the concentrations of 4-DAMP (2 nM) to block I_{KTMA} and of Trop (200 nM) to block I_{K4AP}. Finally, the fact that cDNA fragments representing m_2, m_3, and m_4 isoforms were isolated from

canine atrium and that expression of mRNAs coding for M_2, M_3, and M_4 subtypes was detected by RT-PCR adds an additional evidence for the presence of $M_2/M_3/M_4$ mAChRs in the canine atrium.

Our conclusion relies largely on pharmacological dissection, and false interpretation could have been drawn due to imperfect specificity of mAChR antagonists currently available. Nevertheless, similar approach has been widely used for identifying and classifying mAChR subtypes. Moreover, our conclusion of multiple subtypes of mAChR was further supported by the results from molecular cloning and mRNA expression. No attempt was made to study m_5 subtype in this work because there are no m_5 subtype-selective antagonists available at this time and the potential physiological counterpart is still unknown.

mAChRs have been shown to coupled to several different ion channels. Interaction of M_2 with I_{KACh} probably is the best known example. Other examples include M_2 coupling to a nonselective cation current in smooth muscle cells (Wang et al., 1997) and m_4 coupling to a cloned inward rectifier K^+ channel, GIRK1 (Gadbut et al., 1996). We found here that both M_3 and M_4 are coupled to K^+ channels that possess biophysical and pharmacological characteristics different from other K^+ currents. Neither of the currents are sensitive to dofetilide, indapamide, and 293B, suggesting minimal contribution of the classic delayed rectifier K^+ currents I_{Kr} and I_{Ks} (Wang et al., 1994). Both currents are completely suppressed by atropine and the mAChR subtype-selective antagonists, effects requiring activation of mAChRs. The two channels conduct both outward currents with characteristics of delayed rectifier currents on depolarization and inward currents similar to inward rectifier K^+ currents in response to hyperpolarizing pulses. It is possible that these currents represent integral of two separate populations of channels: one conducting the delayed rectifier-like outward current and the other conducting the inward K^+ current. I_{KTMA} and I_{K4AP} have many differences and similarities as well in terms of their voltage-dependence and kinetics. Whether they represent a single entity or two separate populations of channels is not clear at this time. Although further investigation is absolutely necessary for answering the questions raised above, the issue is beyond the scope of this study.

Our binding experiments showed that both TMA and 4AP were able to displace in a competitive manner the binding of [^{3}H]NMS to mAChRs. The low-affinity K_d value of TMA binding (2.5 mM) is almost identical with the value (2.2 mM) for cloned m_3 receptor reported by Wess et al. (1992). In addition, the K_d values of TMA and 4AP for receptor binding were well coincided with the concentrations of these compounds required for current induction (Table 2).

TMA has been reported to slow the sinus rate and to weaken the contraction of rat hearts (Zakharov et al., 1993). Our results revealed a possible mechanism underlying, at least in part, the TMA-produced negative inotropic and chronotropic effects. TMA activates I_{KTMA}, which should cause hyperpolarization of the membrane and shortening of the action potential duration. Hyperpolarization of membrane could lead to diminished automaticity, thereby slowing heart rate. On the other hand, shortening of action potential would indirectly decrease calcium entry into the cell, which can in turn result in reduction of contractile. 4AP has been reported to induce a delayed rectifier-like K^+ current in isolated cat atrial myocytes (Navarro-Polanco and Sànchez-Chapula, 1997), which was antagonized by atropine and probably mediated through a PTX-sensitive G protein, consistent with our findings in canine cells. In addition, although I_{K4AP} in dog has wave form and kinetics different from the 4AP-induced currents in cat, the two currents seem to share many similarities in terms of their pharmacological sensitivity and the voltage-dependent properties. It is quite likely that the feline 4AP-induced current is equivalent to I_{K4AP} in dog and also is mediated by an M_4 receptor.

Our findings raised several questions regarding the M_3 and M_4 receptors in the heart. First, are there any endogenous activators specific for M_3/M_4 subtypes? Our data in this study showed that ACh, in the presence of M_2 antagonist Meth to inhibit M_2 receptors, increased an outward current with properties distinct from I_{KACh} (Fig. 7). Similar effects were observed in 16 of 29 cells. Our preliminary data demonstrate that this outward current is significantly blocked by 2 nM 4-DAMP or 200 nM Trop, indicating the possible role of M_3 or M_4 receptors, or both. One major difficulty of dissecting this component from I_{KACh} is that Meth cannot completely block M_2 without inhibiting M_3/M_4 receptors. Moreover, ACh has been shown to inhibit the 4AP-induced K^+ current (Navarro-Polanco and Sànchez-Chapula, 1997). We do not know at this time why ACh activates the time-dependent outward currents only when M_2 receptors are largely blocked by the antagonists. Our data do not explain why only a certain percentage of cells possesses the outward current (in the presence of ACh and Meth), and we are unable to provide more reliable evidence for the activation of I_{KTMA}/I_{K4AP} by ACh. Many factors might be involved in this effect, including possible allosteric action of ACh binding to the receptors, heterologous desensitization between different subtypes of mAChRs, or possibly other unknown mechanisms. More careful and detailed investigation is absolutely needed to clarify this issue. We have also obtained data indicating that choline, a precursor and metabolite of ACh, is able to activate currents identical with I_{KTMA}, and the action of choline is also mediated by M_3-subtype receptors (unpublished observations). Second, what are the physiological roles of these novel subtypes of mAChRs and their coupled K^+ channels in cardiac functions? We have performed preliminary experiments and acquired data showing that M_3 activation produced significant slowing of the heart rate and shortening of the action potential duration. Obviously, further investigations are warranted to establish the roles of the cardiac M_3 and M_4 subtypes and their coupled K^+ currents. Third, how are M_3 and M_4 receptors coupled to their K^+ channels? Are they coupled directly via G proteins and other membrane-delimited components or indirectly through the cytoplasmic factors? Although it is of great importance to have better understanding of this aspect, it is out of the scope of the present investigation.

In summary, we have obtained strong functional and molecular evidence for the presence of multiple subtypes of mAChRs ($M_2/M_3/M_4$) as well as the physiological functions of these receptor subtypes in the canine heart. The studies described have the potential to affect greatly our thinking about parasympathetic control of the heart. If the presence and importance of M_3 and M_4 receptors are confirmed, we will no longer be able to consider parasympathetic effects on the heart as due to a simple ACh/M_2 interaction. These

findings potentially open up new opportunities for novel insight into the parasympathetic control of heart functions and the interactions between receptor and channel proteins.

Acknowledgments

We thank Drs. Stanley Nattel and Terry Hebert for their critical review and constructive suggestions on the manuscript, XiaoFan Yang for excellent technical assistance, and Caroll Boyer for secretarial help with the manuscript. We also thank Nathalie Ethier for her professional assistance in our radioligand-binding assay.

References

Araujo DM, Lapchak PA and Quirion R (1991) Heterogeneous binding of [^{3}H]4-DAMP to muscarinic cholinergic sites in the rat brain: Evidence from membrane binding and autoradiographic studies. *Synapse* **9:**165–176

Barlow RP and Shepherd MK (1986) A further search for selective antagonists at M_2-muscarinic receptors. *Br J Pharmacol* **89:**837–843.

Bonner TI, Buckley NJ, Young AC and Brann MR (1987) Identification of a family of muscarinic acetylcholine receptor genes. *Science (Wash DC)* **237:**527–532.

Dixon JE and McKinnon D (1994) Quantitative analysis of potassium channel mRNA expression in atrial and ventricular muscle of rats. *Circ Res* **75:**252–260.

Ehlert FJ and Griffin MT (1988) The use of irreversible ligands to inactivate receptor subtypes: 4-DAMP mustard and muscarinic receptors in smooth muscle. *Life Sci* **62:**1659–1664.

Eglen RM, Reddy H and Watson N (1994) Selective inactivation of muscarinic receptor subtypes. *Int J Biochem* **26:**1357–1368.

Eglen RM and Whiting RL (1990) Heterogeneity of vascular muscarinic receptors. *J Auton Pharmacol* **10:**233–245.

Fermini B and Nattel S (1994) Choline chloride activates time-dependent and time-independent K^+ currents in dog atrial myocytes. *Am J Physiol* **266:**C42–C51.

Gadbut AP and Galper JB (1994) A novel M_3 muscarinic acetylcholine receptor is expressed in chick atrium and ventricle. *J Biol Chem* **269:**25823–25829.

Gadbut AP, Riccardi D, Wu L, Hebert SC and Galper JB (1996) Specificity of coupling of muscarinic receptor isoforms to a novel chick inward-rectifying acetylcholine-sensitive K^+ channel. *J Biol Chem* **271:**6398–6402.

Goyal RK (1989) Muscarinic receptor subtypes: Physiology and clinical implications. *N Engl J Med* **321:**1022–1028.

Hulme EC, Birdsall NJ and Buckley NJ (1990) Muscarinic receptor subtypes. *Annu Rev Pharmacol Toxicol* **30:**633–673.

Jeck D, Lindmar R, Loffelholz K and Wanke M (1988) Subtypes of muscarinic receptor on cholinergic nerves and atrial cells of chicken and guinea-pig hearts. *Br J Pharmacol* **93:**357–366.

Kennedy RH, Wyeth RP, Gerner P, Liu S, Fontenot HJ and Seifen E (1995) Tetramethylammonium is a muscarinic agonist in rat heart. *Am J Physiol* **268:**C1414–C1417.

Lambrecht G, Feifel R, Forth B, Strohmann C, Tacke R and Mutschler E (1988) *p*-Fluoro-hexahydro-sila-difenidol: The first $M_{2\beta}$-selective muscarinic antagonist. *Eur J Pharmacol* **152:**193–194.

Lazareno S and Birdsall NJM (1993) Pharmacological characterization of acetylcholine-stimulated [^{35}S]GTP S binding mediated by human muscarinic m_1-m_4 receptors: antagonist studies. *Br J Pharmacol* **109:**1120–1127.

Lazareno S, Buckley NJ and Roberts FF (1990) Characterization of muscarinic M_4 binding sites in rabbit lung, chicken heart, and NG108–15 cells. *Mol Pharmacol* **38:**805–815.

Maeda A, Kubo T, Mishina M and Numa S (1988) Tissue distribution of mRNAs encoding muscarinic acetylcholine receptor subtypes. *FEBS Lett* **239:**339–342.

McKinnon LA and Nathanson NM (1995) Tissue-specific regulation of muscarinic acetylcholine receptor expression during embryonic development. *J Biol Chem* **270:**20636–20642.

Michel AD, Stefanich E and Whiting RL (1989) Direct labeling of rat M_3- muscarinic receptors by [^{3}H]4-DAMP. *Eur J Pharmacol* **166:**459–466.

Michel AD and Whiting RL (1988) Methoctramine, a polymethylene tetraamine, differentiates three subtypes of muscarinic receptor in direct binding studies. *Eur J Pharmacol* **145:**61–66.

Mizushima A, Uchida S, Zhou XM, Kagiya T and Yoshida H (1987) Cardiac M_2 receptors consist of two different types, both regulated by GTP. *Eur J Pharmacol* **135:**403–409.

Mutschler E, Moser U, Wess J and Lambrecht G (1995) Muscarinic receptor subtypes-pharmacological, molecular biological and therapeutical aspects. *Pharm Acta Helv* **69:**243–258.

Navarro-Polanco RA and Sànchez-Chapula JA (1997) 4-Aminopyridine activates potassium currents by activation of a muscarinic receptor in feline atrial myocytes. *J Physiol (Lond)* **498:**663–678.

Navarro-Polanco RA and Sànchez-Chapula JA (1998) Voltage-dependent activation of the muscarinic receptor by choline and tetramethylammonium. *Biophys J* **74:**326

Peralta EG, Ashkenazi A, Winslow JW, Ramachandran J and Capon DJ (1988) Differential regulation of PI hydrolysis and adenylyl cyclase by muscarinic receptor subtypes. *Nature (London)* **334:**434–437.

Peralta EG, Ashkenazi A, Winslow JW, Smith DH, Ramachandran J and Capon DJ (1987) Distinct primary structures, ligand-binding properties and tissue-specific expression of four human muscarinic acetylcholine receptors. *EMBO J* **6:**3923–3929.

Sharma VK, Colecraft HM, Wang DX, Levey AI, Grigorenko EV, Yeh HH and Sheu SS (1996) Molecular and functional identification of m_1 muscarinic acetylcholine receptors in rat ventricular myocytes. *Circ Res* **79:**86–93.

Takano M and Noma A (1997) Development of muscarinic potassium current in fetal and neonatal rat heart. *Am J Physiol* **272:**H1188–H1195.

Tietje KM, Goldman PS and Nathanson NM (1990) Cloning and functional analysis of a gene encoding a novel muscarinic acetylcholine receptor expressed in chick heart and brain. *J Biol Chem* **265:**2828–2834.

Tietje KM and Nathanson NM (1991) Embryonic chick heart expresses multiple muscarinic acetylcholine receptor subtypes: Isolation and characterization of a gene encoding a novel m_2 muscarinic acetylcholine receptor with high affinity for pirenzepine. *J Biol Chem* **266:**17382–17387.

van Zwieten PA and Doods HN (1995) Muscarinic receptors and drugs in cardiovascular medicine. *Cardiovasc Drugs Ther* **9:**159–167.

Wang YX, Fleischmann B and Kotlikoff M (1997) M_2 receptor activation of nonselective cation channels in smooth muscle cells: calcium and G_i/G_o requirements. *Am J Physiol* **273:**C500–C507.

Wang Z, Fermini B and Nattel S (1994) Rapid and slow components of delayed rectifier current in human atrial myocytes. *Cardiovasc Res* **28:**1540–1546.

Wang Z, Kiehn J, Yang Q, Brown AM and Wible BA (1996) Comparison of binding and block produced by alternatively spliced Kv 1 subunits. *J Biol Chem* **271:**28311–28317.

Wang Z, Yue L, White M, Pelletier G, Nattel S (1998) Differential expression of inward rectifier potassium channel mRNA in human atrium versus ventricle and in normal versus failing. *Circulation* **98:**2422–2428.

Watson M, Yamamura HI and Roeske WR (1983) A unique regulatory profile and regional distribution of [^{3}H]pirenzepine binding in the rat provide evidence for distinct M_1 and M_2 muscarinic receptor subtypes. *Life Sci* **32:**3001–3011.

Wess J, Maggio R, Palmer JR and Vogel Z (1992) Role of conserved threonine and tyrosine residues in acetylcholine binding and muscarinic receptor activation: A study with m_3 muscarinic receptor point mutants. *J Biol Chem* **267:**19313–19319.

Yatani A, Mattera R, Codina J, Graf R, Okabe K, Padrell E, Iyengar R, Brown AM and Birnbaumer L (1988) The G protein-gated atrial K^+ channel is stimulated by three distinct G_i alpha-subunits. *Nature (London)* **33:**680–682.

Yue L, Feng J, Gaspo R, Li GR, Wang Z and Nattel S (1997) Ionic remodeling underlying action potential changes in a canine model of atrial fibrillation. *Circ Res* **81:**512–525.

Zakharov SI, Overholt JL, Wagner RA and Harvey RD (1993) Tetramethylammonium activation of muscarinic receptors in cardiac ventricular myocytes. *Am J Physiol* **264:**C1625–C1630.

Send reprint requests to: Zhiguo Wang, Ph.D, Research Center, Montreal Heart Institute, 5000 Bélanger Street East, Montreal, Quebec, Canada H1T 1C8. E-mail: wangz@icm.umontreal.ca